Marine snow formation by the toxin-producing diatom, *Pseudo-nitzschia australis*

Astrid Schnetzer[a,*], Robert H. Lampe[a,b], Claudia R. Benitez-Nelson[c], Adrian Marchetti[b], Christopher L. Osburn[a], Avery O. Tatters[d]

[a] *Department of Marine, Earth and Atmospheric Sciences, North Carolina State University, Raleigh, NC 27695, USA*
[b] *Department of Marine Sciences, University of North Carolina at Chapel Hill, Chapel Hill, NC 27599, USA*
[c] *School of the Earth, Ocean, & Environment, University of South Carolina, Columbia, SC 29208, USA*
[d] *Department of Biological Sciences, University of Southern California, Los Angeles, CA 90089, USA*

ARTICLE INFO

Article history:
Received 25 January 2016
Received in revised form 9 November 2016
Accepted 10 November 2016
Available online xxx

Keywords:
Marine snow
Domoic acid
Pseudo-nitzschia
Toxin flux
Food web

ABSTRACT

The formation of marine snow (MS) by the toxic diatom *Pseudo-nitschia australis* was simulated using a roller table experiment. Concentrations of particulate and dissolved domoic acid (pDA and dDA) differed significantly among exponential phase and MS formation under simulated near surface conditions (16 °C/12:12-dark:light cycle) and also differed compared to subsequent particle decomposition at 4 °C in the dark, mimicking conditions in deeper waters. Particulate DA was first detected at the onset of exponential growth, reached maximum levels associated with MS aggregates (1.21 ± 0.24 ng mL^{-1}) and declined at an average loss rate of ~1.2% pDA day^{-1} during particle decomposition. Dissolved DA concentrations increased throughout the experiment and reached a maximum of ~20 ng mL^{-1} at final sampling on day 88. The succession by *P. australis* from active growth to aggregation resulted in increasing MS toxicity and based on DA loading of particles and known *in situ* sinking speeds, a significant amount of toxin could have easily reached the deeper ocean or seafloor. MS formation was further associated with significant dDA accumulation at a ratio of pDA: dDA: cumulative dDA of approximately 1:10:100. Overall, this study confirms that MS functions as a major vector for toxin flux to depth, that *Pseudo-nitzschia*-derived aggregates should be considered 'toxic snow' for MS-associated organisms, and that effects of MS toxicity on interactions with aggregate-associated microbes and zooplankton consumers warrant further consideration.

1. Introduction

The diatom genus *Pseudo-nitzschia* has gained world-wide attention in coastal waters due to its production of a potent neurotoxin, domoic acid (DA) (i.e., Anderson et al., 2008; Bates and Trainer, 2006; Kudela et al., 2005; Trainer et al., 2012). *Pseudo-nitzschia* assemblages along many coastal regions often contain several species that produce the toxin domoic acid (DA), which causes Amnesic Shellfish Poisoning (ASP) that may lead to vomiting, memory loss, coma or even death in humans (Bates et al., 1989; Wright et al., 1989). Humans typically suffer from ASP after consumption of toxin-laden shellfish (i.e., Costa and Garrido, 2004; Krogstad et al., 2009; Lefebvre et al., 2001). However, filter-feeding planktivorous fish also play a pivotal role as vectors for DA to pelagic top predators that include marine mammals and seabirds (i.e. Fire et al., 2011; Gulland et al., 2002; Scholin et al., 2000). While much progress has been made in understanding the underlying environmental conditions that drive *Pseudo-nitzschia* bloom dynamics in surface waters, especially along the U.S. west coast, (i.e., Kudela et al., 2008; Trainer et al., 2012; Wells et al., 2015), relatively little information is available on the fate of DA as senescent cells aggregate and sink from the euphotic zone (Schnetzer et al., 2007; Sekula-Wood et al., 2009).

Marine snow (MS) particles (>0.5 mm in size), which are typically comprised of phytodetritus, fecal pellets and other dead or living matter, are major vectors for material transport to depth (Alldredge and Silver, 1988; Fowler and Knauer, 1986; Passow et al., 1994). MS is ubiquitous and abundant in surface waters and may range from <1 to 100 aggregates L^{-1} (Simon et al., 2002; Turner, 2015). As these particles sink to depth they can become a major

* Corresponding author.
E-mail address: aschnet@ncsu.edu (A. Schnetzer).

http://dx.doi.org/10.1016/j.hal.2016.11.008

food source for mesopelagic organisms, or, if they reach the seafloor, for benthic species as well (e.g., see review by Turner, 2015). Various microbes (bacteria and protists) colonize MS and reach densities 2–5 orders of magnitude higher than in the surrounding water (Alldredge et al., 1986; Artolozaga et al., 2002; Herndl, 1988), which makes these aggregates a valuable (enriched) food source for zooplankton, that would not be able to efficiently filter microbe-sized prey if it were not associated with MS ('food chain shortcut') (Dilling et al., 1998; Kach and Ward, 2008; Lampitt et al., 1993; Schnetzer and Steinberg, 2002).

In the wake of a phytoplankton bloom, senescent algae are the major source of MS and diatom cells commonly reach the deep-sea floor relatively intact (Alldredge and Silver, 1988; Michaels and Silver, 1988; Smetacek, 1985). Off the Southern California coast, diatoms dominated by DA-containing *Pseudo-nitzschia*, have been detected in sediment traps and sediments as deep as 800 m providing direct evidence of toxin transfer to depth (Schnetzer et al., 2007; Sekula-Wood et al., 2009, 2011). When compared to bloom dynamics in surface waters, results further suggest that toxin-laden material reaches depth rapidly, sinking on the order of $\sim$100 m d^{-1}. In some cases, sinking particles contained over 5 times the regulatory federal limit for DA instituted for shellfish consumption by humans (>20 ppm DA per gram tissue) (Sekula-Wood et al., 2009). A retrospective sediment trap flux study (down to 540 m) within the Santa Barbara Channel (1993–2008) further suggests that sedimentation events are common and increasing in frequency and magnitude coincident with trends in surface algal blooms (Sekula-Wood et al., 2011). Nonetheless, very little is known about the mechanisms that influence DA transport to depth. The concentrations and fluxes of DA measured in sediment traps are likely minimum estimates, as preservation tests have shown substantial loss of DA (as much as 50%) from particles due to sediment trap collection, recovery, and storage prior to analyses (Sekula-Wood et al., 2011). In this study we examined the production and release of DA by the toxic diatom *Pseudo-nitzschia australis* during exponential growth, stationary phase, and the subsequent formation and decomposition of MS. Additionally, we discuss the role that MS formation plays in DA export to depth and for food web interactions.

2. Materials and methods

2.1. Experimental set-up

MS formation (i.e., classified as particles $\geq$0.5 mm in size) was simulated using 2 L roller glass bottles on a Wheaton roller culture apparatus rotating at $\sim$1.5 rpm (Passow, 2014; Shanks and Edmondson, 1989). For this experiment a coastal non-axenic isolate of toxic *P. australis* from the San Pedro Bay area in Southern California was chosen (BC-4A, isolated April 2013 off Palos Verdes Peninsula). *P. australis* is considered to be one of the most-toxic *Pseudo-nitzschia* species found along the US West Coast (Schnetzer et al., 2013; Trainer et al., 2012). Each bottle (n = 31) was inoculated at initial concentrations of $\sim$15 cells mL^{-1} in 0.2 μm-filtered seawater and amended with a F/2 growth media (NCMA, Bigelow) at a 1:100 dilution (i.e., 8 μM nitrate, 0.4 μM phosphate and 1 μM silicic acid; Guillard 1975). The overall duration of the experiment was 10 weeks. The diatom was grown at 16 °C and a 12:12 L:D cycle at $\sim$180 μEinstein m^{-2} s^{-1} under cool white fluorescent light using a culture incubator (Percival Scientific, Iowa) in order to simulate ambient conditions in the mixed layer of California coastal waters. Once MS aggregates formed within the majority of the bottles ($\sim$20 days after cell growth had slowed), incubation temperatures were reduced from 16 to 4 °C and the bottles were kept in complete darkness to mimic environmental conditions observed below the photic zone.

2.2. Sampling

Triplicate bottles were analyzed at the beginning and throughout the experimental phases, which were denoted as lag phase (Lag), exponential growth (Exp), stationary phase/marine snow formation (MS) and particle decomposition (Dec). Prior to sampling, bottles were gently inverted to evenly distribute cells, or later MS flocks, while minimizing particle disruption. Sample timing was guided by subsampling (5 mL from 6 bottles) the algal cultures every 2 to 4 days to determine *in vivo* fluorescence and cell counts. As MS began to form in the majority of roller bottles, *in vivo* measurements were stopped to minimize disruption of newly formed aggregates. Changes in cell densities were used to calculate specific growth rates during exponential growth (Brand et al., 1981). Cell counts (mL^{-1}) were conducted using an Olympus BX53 compound microscope after preservation with acid Lugol's solution (5%) with settling differing volumes depending on growth phase (Utermöhl, 1958).

2.3. Chlorophyll and toxin measurements

At each major time point (whole bottle analyzed), extracted chlorophyll *a* (μg chl *a* L^{-1}) was determined by filtering 50 mL onto a 25 mm Whatman GF/F (Welschmeyer, 1994). Both, *in vivo* fluorescence (in Raw Fluorescence Units or RFU) and extracted chl *a* were measured using a Trilogy Fluorometer (Turner Designs). DA concentrations (ng mL^{-1}) were obtained using an Enzyme-Linked Immuno Sorbent Assay (ELISA) from Mercury Science (Litaker et al., 2008). For particulate DA (pDA) 200 mLs of sample was filtered onto a 0.45 μm GF/F and 10 mL of the filtrate collected to determine dissolved DA (dDA, detection limit 0.1 ng mL^{-1}). Filtration of 200 mL yielded a pDA detection limit of 0.01 ng mL^{-1}. In addition, we used a Solid Phase Adsorption Toxin Tracking (SPATT) method to obtain information on accumulated dDA over varying time periods, from the beginning of the experiment to the time each bottle was sacrificed (Lane et al., 2010). The SPATT units, which have been used successfully to derive an accumulated dissolved toxin signal in the field, were fit below the caps of the roller bottles and dDA recovered following previously established protocols for column extraction (Lane et al., 2010). The final concentrations were measured using the ELISA method (ng DA [g resin]$^{-1}$). All DA samples were temporarily stored at −80 °C prior to analyses. Cellular DA (cDA in pg $cell^{-1}$) was calculated from total abundances of *P. australis* and pDA concentrations.

2.4. Inorganic nutrients and elemental ratios

Dissolved inorganic nutrient samples (15 mL) were collected after pre-filtration through a 0.45 μm GF/F and stored at −80 °C until analyses of NH_4 and $NO_3 + NO_2$ (each in μM) using a Lachat QuickChem FIA +8000 series following established sampling protocols (Lachat QuikChem methods). Lower limits of detection were 0.04 and 0.01 μM for NH_4, and $NO_3 + NO_2$, respectively. Phosphate or soluble reactive phosphorus (SRP) concentrations were determined colorimetrically (Koroleff, 1983) with a detection limit 0.07 μM. Particulate nutrient samples (200–300 mL) were collected using precombusted 0.45 μm GF/F and stored at −80 °C prior to analysis. Particulate carbon (PC) and particulate nitrogen (PN) concentrations were determined following previously published procedures (Froelich, 1980). Briefly, each filter was wrapped in methanol cleaned tin boats and combusted at 1000 °C in a Perkin Elmer 2400 elemental analyzer. Total particulate phosphorus (TPP) was determined using a modification of the Aspila method, where filters were combusted at 550 °C to convert any organic P to inorganic P, and extracted using a weak hydrochloric acid (Aspila et al., 1976; Benitez-Nelson et al., 2007).

2.5. Statistical analyses

A non-parametric Kruskal-Wallis test was used to analyze whether toxin levels (pDA, dDA and cellular DA) and nutrient ratios (C:N, C:P and N:P) differed throughout the duration of the experiment (McDonald, 2014). Samples that fell below detection limits for nutrient and DA analyses were assigned zeros. Correlation analyses between cell concentrations and toxin levels (cDA, pDA and dDA) with chl *a*, inorganic nutrient concentrations and nutrient ratios were conducted using the software package Statistica (StatSoft, 2002).

3. Results

3.1. Diatom growth and marine snow formation

A time lag was observed in algal growth response throughout the bottles during the first week of the experiment (Days 1–6; see cell densities in Fig. 1A), followed by Exp growth (Days 7–20), stationary phase and MS formation (Days 21 45) and particle Dec (Days 46 to 88). During Exp growth, maximum cell abundances were reached (632 ± 62 cells mL^{-1}) by Day 20 (n = 3, Fig. 1 and Table 1) with a specific growth rate (μ) of 0.97 d^{-1}. Cell abundances were positively correlated with concentrations of extracted chl *a* (r = 0.86, Table 2) and reached a maximum of 46 $\mu g\, L^{-1}$ during late Exp phase. Small-sized MS aggregates (~0.5 mm) were observed as early as late Exp growth (Fig. 2A). Therefore, we did not distinguish between the onset of stationary phase fluently transitioned into MS formation. The number of aggregates formed continued to increase in all bottles and by Day 45, particle sizes of ~4 mm were common (longest dimensions, Fig. 2 B and C). We did not conduct individual aggregate counts for each of the bottles, but densities of 50 60 aggregates L^{-1} were estimated based on images taken during late MS formation (e.g., Fig. 2C). Approximately ~3.5 weeks after cell growth had slowed, incubator conditions were switched from the initial 16 °C/L:D cycle to a 4 °C/completely dark regime to simulate particle decomposition within the aphotic zone. Three more time points were sampled during this stage on Days 63, 74 and 88 (Fig. 1). These final three time points were single bottle observations.

3.2. Particulate and dissolved DA concentrations

Concentrations for pDA ($H = 24.98$, 3 d.f., $p < 0.0001$), dDA ($H = 18.3$, 3 d.f., $p = 0.0004$) and cDA ($H = 22.03$, 2 d.f., $p < 0.0001$) differed significantly (Kruskal-Wallis test) among the varying stages of the experiment (i.e., Lag, Exp, MS and Dec) (Fig. 1 and Table 1). Particulate DA was first detected at the onset of Exp growth (~day 6) with concentrations of 0.07 ± 0.03 ng mL^{-1} (n = 3) and reached a maximum of 1.21 ± 0.24 ng mL^{-1} (n = 6) with MS

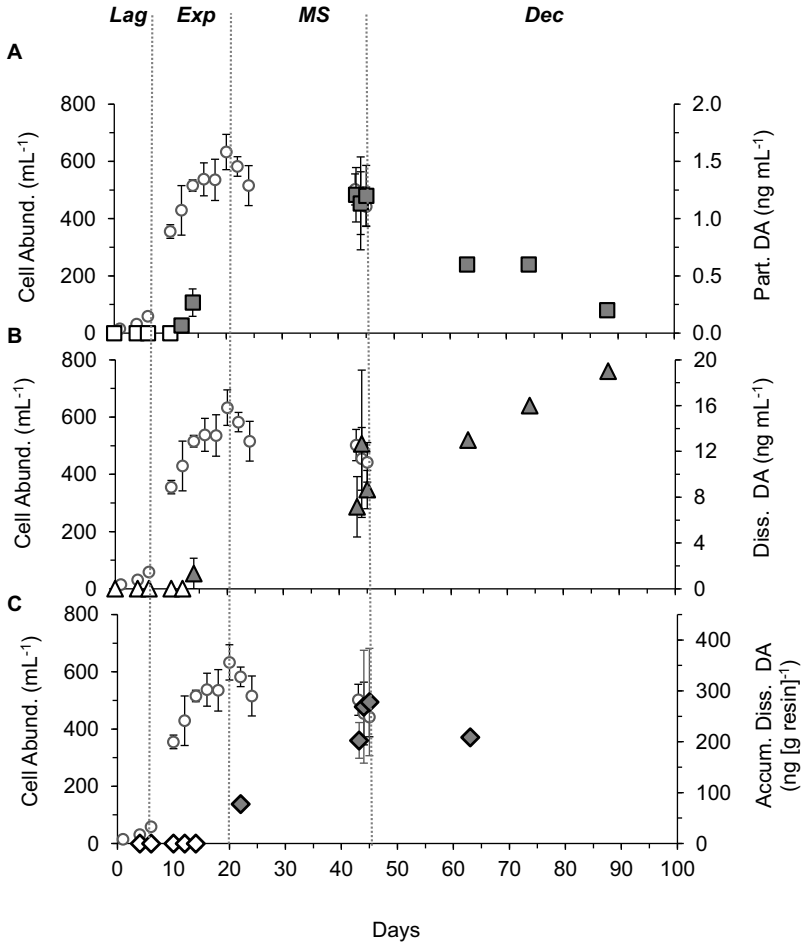

Fig. 1. Cell abundances (cells mL^{-1}; circles) in relation to (A) pDA in ng mL^{-1}, (B) dDA in ng mL^{-1} and (C) accumulated toxin extracted from SPATT units normalized per gram resin (Accum. dDA in ng mL^{-1} [g resin]$^{-1}$). Empty symbols indicate DA analyses were below detection. All results are shown as average with their standard errors (±SE) for triplicate bottles. Time points collected after day 60 were single observations. Dotted lines depict varying phases of the experiment with an initial lag (Lag), exponential growth (Exp), marine snow formation (MS) and particle decomposition (Dec) (see further details text).

Table 1
Summary of cell densities, toxin levels (pDA, dDA, Accum. dDA and cDA), chl *a* concentrations and molar particulate ratios (C:N, C:P and N:P) for each of the experimental stages. Lag = lag phase (n = 9); Exp = exponential growth (n = 9); MS = stationary phase and marine snow formation (n = 12); Dec = particle decomposition (n = 3). Values are listed as average with their standard error (Ave ± SE). Three single observations are denoted by "*", one at each time point, collected during Dec. nd = no cell counts are available.

	Days	Abund. cell mL-1		pDA ng mL^{-1}		dDA ng mL^{-1}		Accum. dDA ng [g resin]$^{-1}$		cDA pg $cell^{-1}$		Chl *a* $\mu g\,L^{-1}$		C:N		C:P		N:P	
		Ave	±SE	Ave	±SE	Ave	±SE	Ave	±SE	Ave	±SE	Ave	±SE	Ave	±SE	Ave	±SE	Ave	±SE
Lag	1 to 6	35	8	0.0	0.0	0.0	0.0	0	0	0.0	0.0	1.7	0.5	4.8	2.0	19	8	4.0	1.8
Exp	7 to 20	433	35	0.1	0.1	0.4	0.4	0	0	0.2	0.1	30.4	3.0	6.7	3.9	38	22	5.6	3.2
MS	21 to 45	475	39	1.2	0.2	8.9	2.0	238	38	2.7	0.5	16.0	2.4	9.0	3.7	59	24	6.5	2.7
Dec*	> 63	nd		0.5	0.1	16.0	1.7	209		nd		25.7	0.8	7.4	4.3	36	21	5.0	2.9

Table 2
Results from linear regression analyses. Individual correlations between cell abundances, cDA, pDA and dDA concentrations with chl *a* (n = 30), inorganic nutrients levels (n = 30) and particulate nutrient ratios (n = 15). Values shown in bold are significant at $p < 0.05$.

	Chl *a*	NH4	NO3 + NO2	PO4	NO3 + NO2: NH4	C: N	C: P	N: P
Cell Abund.	0.764	0.312	−0.740	**−0.793**	**−0.888**	**0.875**	**0.746**	0.604
cDA	−0.439	**−0.497**	**−0.668**	nd	**−0.701**	**0.677**	**0.743**	0.614
pDA	−0.427	**−0.535**	**−0.509**	nd	**−0.524**	**0.641**	**0.664**	0.523
dDA	−0.115	0.030	−0.414	nd	−0.403	−0.358	−0.152	−0.012

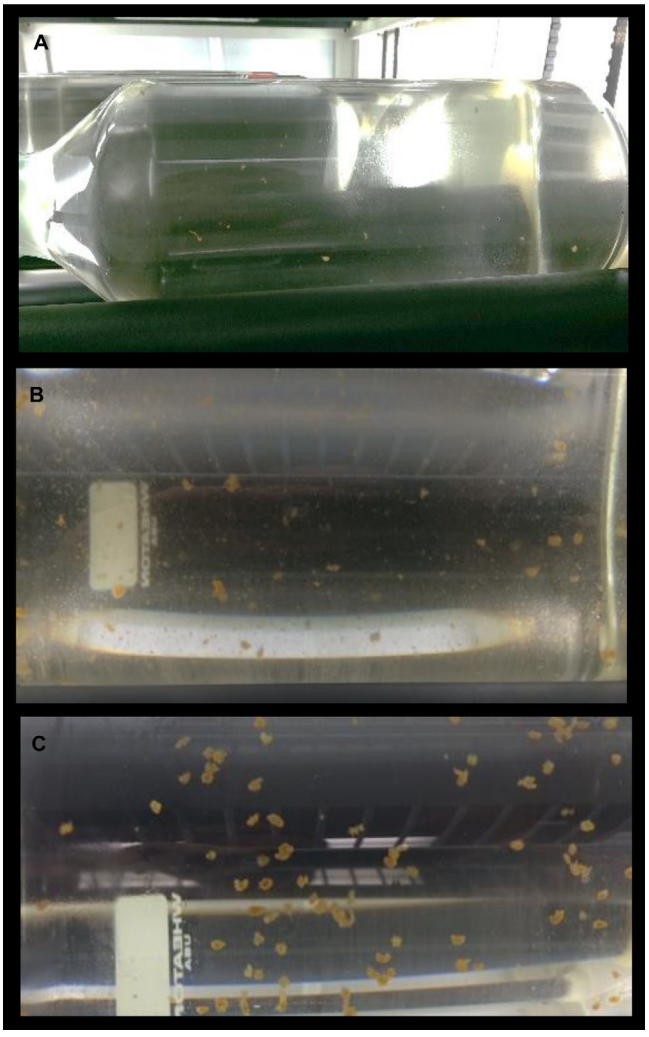

Fig. 2. Roller bottles during varying stages of the experiment showing (A) *P. australis* growth in late Exp phase (day 18), (B and C) during MS formation (days 30 and 40).

formation (~day 45, Fig. 1A). Dissolved DA was first observed on Day 14 (1.33 ng mL^{-1}, n = 1) and, similar to pDA, increased until maximum aggregate sizes were reached, with average concentrations of 7.7 ± 2.64 ng mL^{-1} (n = 6) (Fig. 1B). Within 4 weeks of switching conditions to a 4 °C/dark regime, pDA levels declined to 0.6 ng mL^{-1}, reaching a final concentration of 0.2 ng mL^{-1} after 6 weeks (51 and 17% of initial pDA levels). Meanwhile, dDA continued to increase, reaching a maximum of 19 ng mL^{-1} by the final time point on Day 88 (Fig. 1A and B). The average amount of DA that could have been released into the surrounding water based on the decrease in pDA over the course of the experiment, is only 11% of the dDA measured by discrete sampling. Cumulative dDA levels based on SPATT units were in good agreement with the trend observed for dDA measured from discrete sampling, with concentrations peaking at 224 ± 69 ng [g resin]$^{-1}$ (overall range = 0 –484 ng [g resin]$^{-1}$; n = 29) (Fig. 1C). Cellular DA concentrations were calculated from pDA and cell counts and followed the same trend as pDA, ranging from 0 to 7.7 pg DA $cell^{-1}$ (average = 2.0 pg DA $cell^{-1}$, n = 17).

3.3. Nutrient dynamics and elemental stoichiometry

Growth and toxin dynamics were examined for their relationships with dissolved inorganic nutrients (PO_4, $NO_3 + NO_2$ and NH_4^+) as well as particulate and dissolved nutrient ratios (C:N, C:P and N:P). Cell growth was concurrent with a drawdown in both $NO_3 + NO_2$ ($r = -0.740$, n = 30, $p < 0.05$) and PO_4 concentrations and an increase in particulate C:N ($r = 0.875$, n = 15, $p < 0.05$) and C:P ratios ($r = -0.746$, n = 14, $p < 0.05$; Table 2). PO_4 and $NO_3 + NO_2$ concentrations decreased rapidly as cell abundances increased during the Exp phase (Fig. 3). PO_4 levels declined from an initial concentration of 0.7 ± 0.1 μM (n = 3) to < 0.07 μM by Day 10 (Fig. 3). $NO_3 + NO_2$ concentrations decreased from ~4 to <0.7 μM by late Exp phase and continued to gradually decrease throughout the remainder of the experiment (Fig. 3). NH_4 concentrations showed an initial increase from 1.1 ± 0.1 μM (n = 3) to 1.9 ± 0.1 μM (n = 3) around Day 14 followed by a gradual increase to 2.4 μM during the final sampling period (Fig. 3). The results of Kruskal-Wallis indicated that particulate molar ratios for C:N (H = 15.3, 3 d. f., p = 0.0016) and C:P (H = 13.4, 3 d.f., p = 0.0038) differed significantly among Lag phase, Exp growth, MS formation and

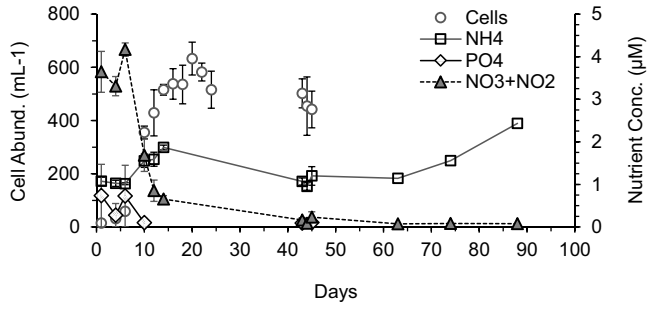

Fig. 3. Cell abundances (cells mL^{-1}) in relation to concentrations (µM) for PO_4^{3-}, $NO_3^- + NO_2^{2-}$ and NH_4^+ throughout the 10-week experiment. Values are shown as averages ± standard error (±SE).

particle Dec (Table 1). Particulate N:P ratios over the varying stages of the experiment, however, were not statistically different (Table 1). Overall, particulate molar C:N ratios ranged from 4 to 10, C:P from 14 to 92, N:P from 3 to 10 and dissolved $NO_3 + NO_2$:NH_4 ratios from 5 to <0.3 (Table 1). Toxin analyses showed that cDA, pDA but not dDA were inversely correlated with NH_4 ($r = -0.497$ ($n = 17$) and -0.535 ($n = 20$), respectively; $p < 0.05$), $NO_3 + NO_2$ ($r = -0.668$ ($n = 17$) and -0.509 ($n = 20$), respectively; $p < 0.05$) and N:NH_4 ratios ($r = -0.701$ ($n = 17$) and -0.524 ($n = 20$), respectively; $p < 0.05$, Table 2 and Fig. 4A–C). Both cDA and pDA were also positively correlated with particulate C:N ($r = 0.677$ ($n = 8$) and 0.641 ($n = 10$), respectively; $p < 0.05$) and C:P ratios ($r = 0.743$ and 0.664 ($n = 10$), respectively; $p < 0.05$, Table 2and Fig. 4D and E). No correlation was seen with particulate N:P ratios (Table 2 and Fig. 4D–F). Initial dissolved $NO_3 + NO_2$:P ratios averaged ~7.8 ($n = 6$) and dropped to <2 by the time MS formed ($n = 2$; only a few ratios could be calculated since the majority of PO_4 concentrations fell below the detection limit (BD) after day 12).

4. Discussion

4.1. Domoic acid levels associated with cell growth, aggregate formation and decomposition

Toxin dynamics were closely linked to Exp growth (active growth), stationary phase and MS formation, and particle decomposition. *P. australis* abundance with up to ~600 cells mL^{-1}, and pDA, dDA, and cDA concentrations (BD – 2.0 ng mL^{-1}, BD – 21 ng mL^{-1}, and BD – 7.7 pg DA $cell^{-1}$) were similar to those observed during major toxic events along the California coast (e.g., Schnetzer et al., 2013; Scholin et al., 2000; Trainer et al., 2000). Considerable research has been conducted to understand the environmental and biological factors that are responsible for the onset and magnitude of DA production (e.g., macro- and micronutrient limitation) (i.e., see reviews in (Bates et al., 1995; Tatters et al., 2012; Trainer et al., 2012), but there is likely a suite of conditions (stressors) that induce toxicity in varying *Pseudo-nitzschia* species. Based on the available data in this study, the onset of DA production by *P. australis* was correlated with decreases in PO_4 and $NO_3 + NO_2$ (namely NO_3), which corroborates toxin concentrations (pDA and dDA) being positively associated with increasing particulate C:N and C:P ratios (Table 2). While no relationship between toxin dynamics and particulate N:P ratios was detected, dissolved $NO_3 + NO_2$:P ratios declined to <2 during MS formation, suggesting limitation. A concurrent strong decrease in $NO_3 + NO_2$:NH_4 ratios further pointed to the importance of remineralized NH_4 as a major nitrogen source for toxin production during particle formation. These results are consistent with culture and *in situ* data that link low N:P waters and high NH_4

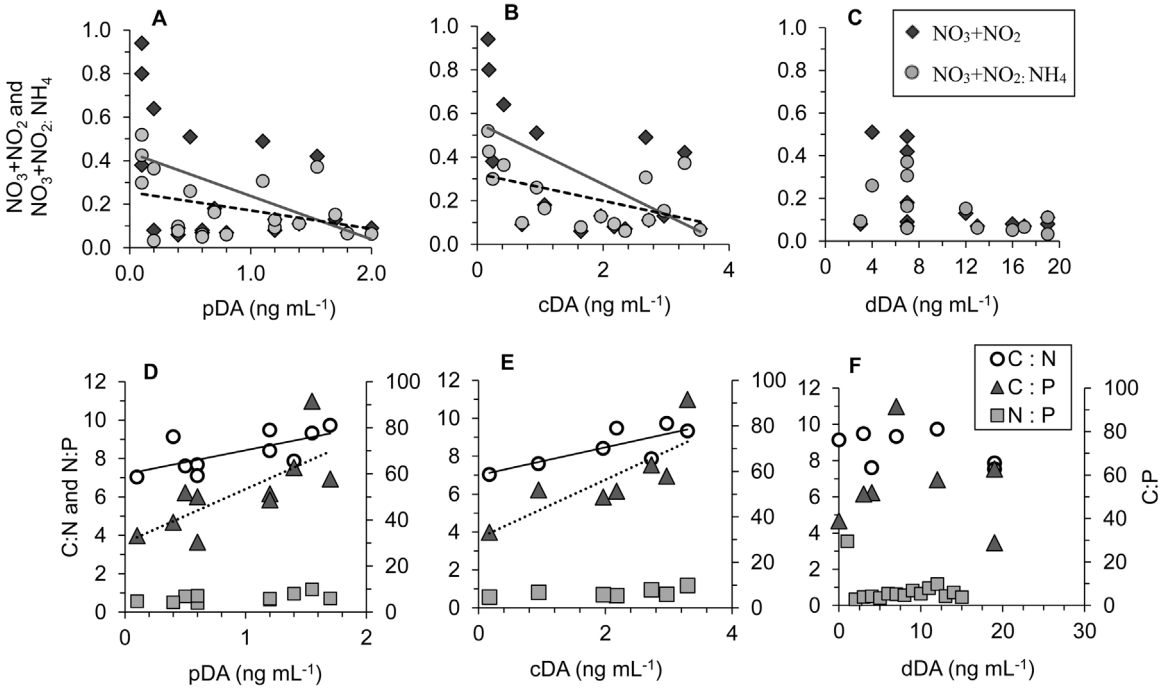

Fig. 4. Toxin levels in relation to dissolved $NO_3 + NO_2$ and $NO_3 + NO_2$:NH_4 ratios (panels A-C) and to C:N, C:P and N:P molar particulate ratios (panels D-F). Cellular DA (cDA) was inversely correlated with $NO_3 + NO_2$ (dashed regression line; $R^2 = 0.25$) and $NO_3 + NO_2$:NH_4 (solid grey line, $R^2 = 0.33$, respectively, panel A). Particular DA (pDA) was also weakly correlated with $NO_3 + NO_2$ ($R^2 = 0.25$) and $NO_3 + NO_2$:NH_4 ($R^2 = 0.13$, panel B), but no relationship confirmed for dissolved DA (dDA, panel C). CDA was positively correlated with C:N (solid regression line; $R^2 = 0.38$) and C:P (dotted line, $R^2 = 0.70$,) but not N:P (panel D). Similarly, pDA was positively correlated with C:N ($R^2 = 0.46$) and C:P ($R^2 = 0.54$) but not N:P (panel E). No significant relationships detected for dDA panel F).

concentrations to toxin production in *Pseudo-nitzschia* species (e.g., Bograd et al., 2015; Kaltenboeck and Herndl, 1992; Schnetzer et al., 2013).

Particulate DA and dDA reached their highest concentrations when associated with MS and contributions of dDA to total toxin (dDA + pDA) were significant (71–99%) throughout the experiment. Within ~3 weeks of particles being formed, the incubator temperature was reduced from an initial 16 °C, representative for the mixed layer in California coastal waters (Kim et al., 2014), to 4 °C in the dark to simulate conditions below the euphotic zone (e.g., > 300 m) over an additional 6 weeks. MS-associated pDA levels dropped to 17% while dDA concentrations continued to gradually increase to ~20 ng mL^{-1} (Fig. 1C). Comparison of the loss of pDA with the increase of dDA during this phase, indicated that only 11% of the dissolved toxin in the surrounding water originated from within senescent cells or MS aggregates. Thus, the remaining dDA had accumulated over the duration of the experiment. Our results suggest that dDA persisted throughout the various growth phases of *P. australis* as well as beyond the duration of the experiment. While the sampling itself may have caused some of the dissolved toxin to leak from senescent cells or aggregates, results from this study are in good agreement with laboratory studies that reported high proportions of dDA (pDA:dDA ≈ 1:10) during Exp and stationary phases under trace metal stress (Maldonado et al., 2002; Wells et al., 2005). Moreover, ~88% of DA in sediment traps, likely derived from MS sinking to 540 m depth, was detected in its dissolved form (Sekula-Wood et al., 2011). Overall, MS aggregates were associated with a ratio of pDA: dDA: cumulative dDA of ≈ 1:10:100. We believe that these findings warrant further consideration in future research, given that the vast majority of *Pseudo-nitzschia* studies to date have focused solely on toxin production during Exp and stationary phases and often do not consider DA in its dissolved form.

4.2. Domoic acid export due to marine snow formation

Diatom aggregation is often the primary source of MS (Alldredge et al., 1995; Thornton, 2002). The timing of sedimentation and *in situ* sinking rates of these particles govern carbon export, and in case of *Pseudo-nitzschia*, DA fluxes to depth. Both processes depend on several factors including particle composition (e.g., contributions from transparent exopolymer particles (TEP) or fecal pellets) (Alldredge et al., 1995; Passow et al., 2012; Shanks and Trent, 1980), microbial interactions (Gärdes et al., 2011; Heissenberger et al., 1996; Vojvoda et al., 2014) and physical conditions (e.g., turbulence, temperature) (Bach et al., 2012; Burd and Jackson, 2009; Kioerboe, 1997). Delays in settling may occur if flocks accumulate along physical gradients (i.e., subsurface layers or surface) (Herndl and Peduzzi, 1988; Rines et al., 2002; Schnetzer et al., 2013) and prolonged residence times ≥2 weeks, have been reported in the field (Alldredge et al., 1987; Riebesell, 1992). As for MS in general, extended time in surface waters may allow less material to settle as remineralization and decomposition take place in the near surface, and, in the case of DA, may also prolong the time period for photochemical degradation (mainly due to UVA-exposure) once DA has been released into the surrounding water (Bouillon et al., 2008, 2006; Zabaglo et al., 2016).

In this study, the succession by *P. australis* from active growth to aggregation resulted in sinking toxic MS of 1- 4 mm size, aggregate sizes for which settling speeds of ≥ 100 m d^{-1} have been reported from both laboratory and field observations (Alldredge and Silver, 1988; Diercks and Asper, 1997; Shanks and Trent, 1980). We calculated a pDA loss rate of 1.7% d^{-1} over the first 4 weeks at 4 °C, declining to 1.2% over weeks 5 and 6. Considering these rates and sinking speeds of ~100 m d^{-1}, a significant amount of MS-associated toxin (>80%) could have easily reached sediment traps at 500 m and deeper in the Santa Barbara Basin and San Pedro Bay. While we cannot link the specific contributions of MS-associated DA to sinking particles for flux rate estimates, we can compare the concentrations found in the aggregation experiment with that found in sediment traps. The MS-associated pDA levels, normalized per unit carbon, averaged 372 ng pDA mg C^{-1} and ranged from 168 to 633 ng mg C^{-1}. These values compare well with DA loads for sediment-trap material at 540 m depth in the Santa Barbara Basin, which averaged 27 ng pDA mg C^{-1}, and ranged from <1–882 ng mg C^{-1} (only includes samples positive for DA; Sekula-Wood et al., 2011; Umhau et al., in prep). As mentioned, MS formation in the roller bottles was also associated with significant dDA accumulation that peaked at 480 ng [g resin]$^{-1}$. Comparable integrated dDA levels over 2-week periods were reported from sediment trap supernatant recovered from 540 m depth (Sekula-Wood et al., 2011). These values commonly exceeded 600 ng mL^{-1} and reached up to 4190 ng mL^{-1} (Sekula-Wood et al., 2011). Overall, these findings suggest, that *Pseudo-nitzschia*-derived aggregates could be considered "toxic snow" for aggregate-associated organisms and that slow release of DA from particles will provide chronic exposure to the toxin.

4.3. Marine snow toxicity and possible food web implications

There is a growing body of evidence that MS-associated organisms may be exposed to significant levels of DA following the demise of a toxic *P. australis* bloom (Sekula-Wood et al., 2011, 2009; this study). Culture studies show that bacterial composition can be linked to whether a toxic or non-toxic strain is the host (Lelong et al., 2014; Sison-Mangus et al., 2014). Furthermore, bacteria may play a role in instigating toxin production during late Exp and stationary phase (e.g., Bates et al., 1995; Kaczmarska et al., 2005; Sison-Mangus et al., 2014). Once aggregates are formed and recycled, complex changes in both community dynamics and productivity for MS-associated microbes have been demonstrated (e.g., Gram et al., 2002; Kiørboe et al., 2003; Kramer et al., 2016; Vojvoda et al., 2014). The release of high-molecular-weight polymers by decaying phytoplankton are associated with increasing microbial densities (2–5 fold compared to surrounding water) and an increasing number of microzones that are characterized by varying biogeochemical gradients (e.g., oxygen or nutrient concentrations) (Bochdansky et al., 2010, 2013; Kaltenboeck and Herndl, 1992; Kramer et al., 2016; Silver et al., 1978). Conceivably, DA loading associated with differently-aged MS could further affect these particle-microbe dynamics.

MS plays an important role in the diet of zooplankton, both pelagic and benthic. Several studies have shown that benthic suspension feeders as well as open ocean diel vertical migrants feed on MS (Bochdansky and Herndl, 1992; Kach and Ward, 2008; Lampitt et al., 1993; Lyons et al., 2005; Schnetzer and Steinberg, 2002). Zooplankton feeding activities could negatively affect export of pDA due to MS fragmentation or, alternatively, could be seen as enhancing flux if DA is incorporated into fast-sinking fecal pellets (Goldthwait et al., 2004; Graham et al., 2000; Tammilehto et al., 2012). Based on a few laboratory experiments using *Pseudo-nitzschia* cultures, DA concentration does not cause copepods to choose non-toxic over toxic cells (Lincoln et al., 2001; Maneiro et al., 2005; Tester et al., 2001). However, Bargu et al. (2006) showed that the presence of dDA at levels comparable to those observed during MS formation in this study, negatively affected krill consumption rates (Bargu et al., 2006). Although DA body burdens for krill make them likely vectors for DA to higher trophic levels (i.e. anchovies, Lefebvre et al., 2001), dDA "threshold concentrations" associated with MS may deter krill (and other zooplankton) feeding, which may both positively and negatively

influence the magnitude of toxin-laden fluxes that reach the seafloor.

Our current state of knowledge argues that benthic organisms are exposed to significant algal toxin loads. Within benthic environments from 15 to ~180 m depth, burrowing crustaceans, worms and bottom-dwelling fish have tested positive for DA, with their body burdens repeatedly exceeding the regulatory limit instituted for shellfish consumption by humans (>20 ppm or μg DA per gram tissue) (Kvitek et al., 2008; Vigilant and Silver, 2005, 2007). As toxin flux to benthic communities is expected to increase in frequency and magnitude (Sekula-Wood et al., 2011), so may the risk for human exposure to DA through commercially-marketed benthic shellfish and fish (i.e. halibut; Kvitek et al., 2008). Along the US West Coast, a recent *Pseudo-nitzschia* bloom of unprecedented magnitude and toxicity, was linked to record levels of the toxin in benthic species such as razor clams and Dungeness crabs (R. Kudela, pers. communication). The fact that such levels are reported months after blooms vanished from surface waters further supports the importance of deciphering the mechanisms that underlie DA flux to the seafloor. Based on this study's findings, a better predictive understanding of how DA events impact both pelagic and benthic systems will require consideration of how DA dynamics are influenced by MS formation and whether MS toxicity alters biogeochemical cycling by aggregate-associated microbes and zooplankton.

Acknowledgements

This research has been partially funded by grants 1459406 and 0850425 through the National Science Foundation, by SEED money from North Carolina Sea Grant (NA10OAR1040080) and an undergraduate fellowship by the Division of Academic & Student Affairs at North Carolina State University. Thanks to A. Fowler and R. Duke for assistance during the experiment. We thank J. Bursey for help with the experimental setup and helpful suggestions on SPATT analyses from R. Kudela and K. Negrey. We also thank the anonymous reviewers for their insightful comments and suggestions.

References

Alldredge, A.L., Silve, M.W., 1988. Characteristics, dynamics and significance of marine snow. Prog. Oceanogr. 20 (1), 41–82.
Alldredge, A.L., Cole, J.J., Caron, D.A., 1986. Production of heterotrophic bacteria inhabiting macroscopic organic aggregates (marine snow) from surface waters. Limnol. Oceanogr. 31 (1), 68–78.
Alldredge, A.L., Gotschalk, C.C., MacIntyre, S., 1987. Evidence for sustained residence of macrocrustacean fecal pellets in surface waters off Southern California. Deep-Sea Res. 34 (9), 1641–1652.
Alldredge, A.L., Gotschalk, C., Passow, U., Riebesell, U., 1995. Mass aggregation of diatom blooms: insights from a mesocosm study. Deep Sea Res. Part II: Topical Stud. Oceanogr. 42 (1), 9–27.
Anderson, M.J., Gorley, R.N., Clarke, K.R., 2008. PERMANOVA+ for PRIMER: Guide to Software and Statistical Methods. PRIMER-E, Plymouth, UK.
Artolozaga, I., Valcarecel, M., Ayo, B., Latatu, A., Iriberri, J., 2002. Grazing rates of bacterivorous protists inhabiting diverse marine planktonic microenvironments. Limnol. Oceanogr. 47 (1), 142–150.
Aspila, K.I., Agemian, H., Chau, A.S.Y., 1976. A semi-automated method for the determination of inorganic, organic and total phosphate in sediments. Analyst 101 (1200), 187–197.
Bach, L., Riebesell, U., Sett, S., Febiri, S., Rzepka, P., Schulz, K., 2012. An approach for particle sinking velocity measurements in the 3–400 μm size range and considerations on the effect of temperature on sinking rates. Mar. Biol. 159 (8), 1853–1864.
Bargu, S., Lefebvre, K., Silver, M.W., 2006. Effect of dissolved domoic acid on the grazing rate of krill *Euphausia pacifica*. Mar. Ecol. Progr. Ser. 312, 169–175.
Bates, S.S., Trainer, V.L., 2006. The ecology of harmful diatoms. In: Graneli, E., Turner, J.T. (Eds.), Ecology of Harmful Algae. Springer, Berlin, pp. 81–93.
Bates, S.S., Bird, C.J., de Freitas, A.S.W., Foxall, R., Gilgan, M., Hanic, L.A., Johnson, G.R., McCulloch, A.W., Dodense, P., Pocklington, R., Quilliam, M.A., Sim, P.G., Smith, J. C., Subba Rao, D.V., Todd, C.D., Walter, J.A., Wright, J.L.C., 1989. Pennate diatom Nitzschia pungens as the primary source of domoic acid, a toxin in shellfish from eastern Prince Edwards Island, Canada. Can. J. Fish. Aquat. Sci. 46, 1203–1215.
Bates, S.S., Douglas, D.J., Doucette, G.J., Leger, C., 1995. Enhancement of domoic acid production by reintorducing bacteria to axenic culutres of the diatom *Pseudo-nitzschia multiseries*. Nat. Tox. 3, 428–435.
Benitez-Nelson, C.R., O'Neill Madden, L.P., Styles, R.M., Thunell, R.C., Astor, Y., 2007. Inorganic and organic sinking particulate phosphorus fluxes across the oxic/anoxic water column of Cariaco Basin, Venezuela. Mar. Chem. 105 (1–2), 90–100.
Bochdansky, A.B., Herndl, G.J., 1992. Ecology of amorphous aggregations (marine snow) in the northern Adriatic Sea. 3. Zooplankton interactions with marine snow. Mar. Ecol. Progr. Ser. 87 (1-2), 135–146.
Bochdansky, A.B., van Aken, H.M., Herndl, G.J., 2010. Role of macroscopic particles in deep-sea oxygen consumption. Proc. Nat. Acad. Sci. 107 (18), 8287–8291.
Bochdansky, A.B., Jericho, M.H., Herndl, G.J., 2013. Design and deployment of a point-source digital inline holographic microscope for the study of plankton and particles to a depth of 6000 m. Limnol. Oceanogr. 11, 28–40.
Bograd, S.J., Buil, M.P., Lorenzo, E.D., Castro, C.G., Schroeder, I.D., Goericke, R., Anderson, C.R., Benitez-Nelson, C., Whitney, F.A., 2015. Changes in source waters to the Southern California Bight. Deep Sea Res. Part II 112, 42–52.
Bouillon, R.C., Knierim, T.L., Kieber, R.J., Skrabal, S.A., Wright, J.L.C., 2006. Photodegradation of the algal toxin domoic acid in natural water matrices. Limnol. Oceanogr. 51 (1), 321–330.
Bouillon, R.-C., Kieber, R.J., Skrabal, S.A., Wright, J.L.C., 2008. Photochemistry and identification of photodegradation products of the marine toxin domoic acid. Mar. Chem. 110 (1–2), 18–27.
Brand, L.E., Guillard, R.R.L., Murphy, L.S., 1981. A method for the rapid and precise determination of acclimated phytoplankton reproduction rates. J. Plankton Res. 3 (2), 193–201.
Burd, A.B., Jackson, G.A., 2009. Particle aggregation. Ann. Rev. Mar. Sci. 1 (1), 65–90.
Costa, P.R., Garrido, S., 2004. Domoic acid accumulation in the sardine *Sardina pilchardus* and its relationship to *Pseudo-nitzschia* diatom ingestion. Mar. Ecol. Progr. Ser. 284, 261–268.
Diercks, A., Asper, V.L., 1997. In situ settling speeds of marine snow aggregates below the mixed layer: black Sea and Gulf of Mexico. Deep Sea Res. Part A. Oceanogr. Res. Pap. 44, 385–398.
Dilling, L., Wilson, J., Steinberg, D.K., Alldredge, A.L., 1998. Feeding by the euphausiid Euphausia pacifica and the copepod Calanus pacificus on marine snow. Mar. Ecol. Progr. Ser. 170, 189–201.
Fire, S.E., Wang, Z., Byrd, M., Whitehead, H.R., Paternoster, J., Morton, S.L., 2011. Co-occurrence of multiple classes of harmful algal toxins in bottlenose dolphins (*Tursiops truncatus*) stranding during an unusual mortality event in Texas, USA. Harm. Algae 10 (3), 330–336.
Fowler, S.W., Knauer, G.A., 1986. Role of large particles in the transport of elements and organic compounds through the oceanic water column. Prog. Oceanogr. 16 (3), 147–194.
Froelich, P., 1980. Analysis of organic carbon in marine sediments. Limnol. Oceanogr. 25, 564–572.
Gärdes, A., Iversen, M.H., Grossart, H.-P., Passow, U., Ullrich, M.S., 2011. Diatom-associated bacteria are required for aggregation of *Thalassiosira weissflogii*. ISME J. 5 (3), 436–445.
Goldthwait, S., Yen, J., Brown, J., Alldredge, A., 2004. Quantification of marine snow fragmentation by swimming euphausiids. Limnol. Oceanogr. 49 (4), 940–952.
Graham, W.M., MacIntyre, S., Alldredge, A.L., 2000. Diel variations of marine snow concentration in surface waters and implications for particle flux in the sea. Deep-Sea Res. 147 (3), 367–395.
Gram, L., Grossart, H.-P., Schlingloff, A., Kiørboe, T., 2002. Possible quorum sensing in marine snow bacteria: production of acylated homoserine lactones by *Roseobacter* strains isolated from marine snow. Appl. Environ. Microbiol. 68 (8), 4111–4116.
Gulland, F.M., Fauquier, D., Langlois, G., Lander, M.E., Zabka, T., Duerr, R., 2002. Domoic acid toxicity in Californian sea lions (*Zalophus californianus*): clinical signs, treatment and survival. Vet. Rec. 150, 475–480.
Heissenberger, A., Leppard, G.G., Herndl, G.J., 1996. Ultrastructure of marine snow. II. Microbiological considerations. Mar. Ecol. Progr. Ser. 135, 299–308.
Herndl, G.J., Peduzzi, P., 1988. The ecology of amorphous aggregations (Marine snow) in the northern adriatic sea. Mar. Ecol. 9 (1), 79–90.
Herndl, G.J., 1988. Ecology of amorphous aggregations (marine snow) in the Northern Adriatic Sea. II. Microbial density and activity in marine snow and its implication to overall pelagic processes. Mar. Ecol. Progr. 48, 265–275.
Kach, D.J., Ward, J.E., 2008. The role of marine aggregates in the ingestion of picoplankton-size particles by suspension-feeding molluscs. Mar. Biol. 153 (5), 797–805.
Kaczmarska, I., Ehrman, J.M., Bates, S.S., Green, D.H., Léger, C., Harris, J., 2005. Diversity and distribution of epibiotic bacteria on *Pseudo-nitzschia multiseries* (Bacillariophyceae) in culture, and comparison with those on diatoms in native seawater. Harm. Algae 4 (4), 725–741.
Kaltenboeck, E., Herndl, G.J., 1992. Ecology of amorphous aggregations (marine snow) in the Northern Adriatic Sea. IV. Dissolved nutrients and the autotrophic community associated with marine snow. Mar. Ecol. Progr. 87, 147–159.
Kiørboe, T., Tang, K., Grossart, H.-P., Ploug, H., 2003. Dynamics of microbial communities on marine snow aggregates: colonization, growth detachment, and grazing mortality of attached bacteria. Appl. Environ. Microbiol. 69 (6), 3036–3047.

Kim, D.Y., Countway, P.D., Jones, A.C., Schnetzer, A., Yamashita, W., Tung, C., Caron, D. A., 2014. Monthly to interannual variability of microbial eukaryote assemblages at four depths in the eastern North Pacific. ISME J. 8 (3), 515–530.
Kioerboe, T., 1997. Small-scale turbulence, marine snow formation, and planktivorous feeding. Sci. Mar. (Barc.) 61, 141–158.
Koroleff, F., 1983. Determination of Nutrients. Verlag Chemie, Weinheim.
Kramer, A.M., Ward, J.E., Dobbs, F.C., Pierce, M.L., Drake, J.M., 2016. The contribution of marine aggregate-associated bacteria to the accumulation of pathogenic bacteria in oysters: an agent-based model. Ecol. Evol. 6 (20), 7397–7408.
Krogstad, F.O., Griffith, W., Vigoren, E., Faustman, E., 2009. Re-evaluating blue mussel depuration rates in 'dynamics of the phycotoxin domoic acid: accumulation and excretion in two commercially important bivalves'. J. Appl. Phycol. 21 (6), 745–746.
Kudela, R.M., Pitcher, G., Probyn, T., Figueiras, F., Moita, T., Trainer, V.L., 2005. Harmful algae blooms in coastal upwelling systems. Oceanography 18 (2), 184–197.
Kudela, R.M., Lane, J.Q., Cochlan, W.P., 2008. The potential role of anthropogenically derived nitrogen in the growth of harmful algae in California, USA. Harm. Algae 8 (1), 103–110.
Kvitek, R.G., Goldberg, J.D., Smith, G.J., Doucette, G.J., Silver, M.W., 2008. Domoic acid contamination within eight representative species from the benthic food web of Monterey Bay California, USA. Mar. Ecol. Progr. Ser. 367, 35–47.
Lampitt, R.S., Wishner, K.F., Turley, C.M., Angel, M.V., 1993. Marine snow studies in the Northeast Atlantic ocean: distribution, composition and role as a food source for migrating plankton. Mar. Biol. 116 (4), 689–702.
Lane, J.Q., Roddam, C.M., Langlois, G.W., Kudela, R.M., 2010. Application of Solid Phase Adsorption Toxin Tracking (SPATT) for field detection of the hydrophilic phycotoxins domoic acid and saxitoxin in coastal California. Limnol. Oceanogr. Meth. 8, 645–660.
Lefebvre, K.A., Dovel, S.L., Silver, M.W., 2001. Tissue distribution and neurotoxic effects of domoic acid in a prominent vector species, the northern anchovy Engraulis mordax. Mar. Biol. 138, 693–700.
Lelong, A., Hégaret, H., Soudant, P., 2014. Link between domoic acid production and cell physiology after exchange of bacterial communities between toxic *Pseudo-nitzschia multiseries* and non-toxic *Pseudo-nitzschia delicatissima*. Mar. Drugs 12 (6), 3587–3607.
Lincoln, J.A., Turner, J.T., Bates, S.S., Leger, C., Gauthier, D.A., 2001. Feeding, egg production, and egg hatching success of the copepods *Acartia tonsa* and *Temora longicornis* on diets of the toxic diatom *Pseudo-nitzschia multiseries* and the non-toxic diatom *Pseudo-nitzschia pungens*. Hydrobiology 453 (1-3), 107–120.
Litaker, R.W., Stewart, T.N., Eberhart, B.T.L., Wekell, J.C., Trainer, V.L., Kudela, R.M., Miller, P.E., Roberts, A., Hertz, C., Johnson, T.A., Frankfurter, G., Smith, J., Schnetzer, A., Schumacker, J., Bastian, J.L., Odell, A., Gentien, P., Le Gal, D., Hardison, D.R., Tester, P.A., 2008. Rapid enzyme-linked immunosorbent assay for detection of the algal toxin domoic acid. J. Shellfish Res. 27 (5), 1–10.
Lyons, M.M., Ward, J.E., Uhlinger, K.R., Gast, R.J., Smolowitz, R., 2005. Lethal marine snow: pathogen of bivalve mollusc concealed in marine aggregates. Limnol. Oceanogr. 50 (6), 1983–1988.
Maldonado, M.T., Hughes, M.P., Rue, E.L., Wells, M.L., 2002. The effect of Fe and Cu on growth and domoic acid production by *Pseudo-nitzschia multiseries* and *Pseudo-nitzschia australis*. Limnol. Oceanogr. 47 (2), 515–526.
Maneiro, I., Iglesias, P., Guisande, C., Riveiro, I., Barreiro, A., Zervoudaki, S., Granéli, E., 2005. Fate of domoic acid ingested by the copepod *Acartia clausi*. Mar. Biol. 148 (1), 123–130.
McDonald, J.H., 2014. Handbook of Biological Statistics, third ed. Sparky House Publishing, Baltimore, Maryland.
Michaels, A.A., Silver, M.W., 1988. Primary production, sinking fluxes and the microbial food web. Deep Sea Res. Part A 35, 473–490.
Passow, U., Alldredge, A.L., Logan, B.E., 1994. The role of particulate carbohydrate exudates in the flocculation of diatom blooms. Deep-Sea Res. 41 (2), 335–357.
Passow, U., Ziervogel, K., Asper, V., Diercks, A., 2012. Marine snow formation in the aftermath of the Deepwater Horizon oil spill in the Gulf of Mexico. Environ. Res. Lett. 7 (3), 035301.
Passow, U., 2014. Formation of rapidly-sinking, oil-associated marine snow. Deep Sea Res. Part II: Topical Stud. Oceanogr..
Riebesell, U., 1992. The formation of large marine snow and its sustained residence in surface waters. Limnol. Oceanogr. 37 (1), 63–76.
Rines, J.E.B., Donaghay, P.L., Dekshenieks, M.M., Sullivan, J.M., Twardowski, M.S., 2002. Thin layers and camouflage: hidden *Pseudo-nitzschia* spp. (Bacillariophyceae) populations in a fjord in the San Juan Island, Washington, USA. Mar. Ecol. Progr. Ser. 225, 123–137.
Schnetzer, A., Steinberg, D.K., 2002. Natural diets of vertically migrating zooplankton in the Sargasso sea. Mar. Biol. 141, 89–99.
Schnetzer, A., Miller, P.E., Schaffner, R.A., Stauffer, B.A., Jones, B.H., Weisberg, S.B., DiGiacomo, P.M., Berelson, W.M., Caron, D.A., 2007. Blooms of *Pseudo-nitzschia* and domoic acid in the san pedro channel and los angeles harbor areas of the southern california bight, 2003–2004. Harm. Algae 6 (3), 372–387.
Schnetzer, A., Jones, B.H., Schaffner, R.A., Cetinic, I., Fitzpatrick, E., Miller, P.E., Seubert, E.L., Caron, D.A., 2013. Coastal upwelling linked to toxic Pseudo-nitzschia australis blooms in Los Angeles coastal waters, 2005–2007. J. Plankton Res. 35, 1080–1092.
Scholin, C.A., Gulland, F., Doucette, G.J., Benson, S., Busman, M., Chavez, F., Cordaro, J., Delong, E.F., Vogelaere, A.D., Harvey, J., Haulena, M., Lefebvre, K., Lipscomb, T., Loscutoff, S., Lowenstine, L.J., Marin III, R., Miller, P.E., McLellan, W.A., Moeller, P. D.R., Powell, C.L., Rowles, T., Silvagni, P., Silver, M.W., Spraker, T., Trainer, V.L., Dolah, F.M.V., 2000. Mortality of sea lions along the central California coast linked to a toxic diatom bloom. Nature 403 (6765), 80–84.
Sekula-Wood, E., Schnetzer, A., Benitez-Nelson, C.R., Anderson, C., Berelson, W.M., Brzezinski, M.A., Burns, J.M., Caron, D.A., Cetinic, I., Ferry, J.L., Fitzpatrick, E., Jones, B.H., Miller, P.E., Morton, S.L., Schaffner, R.A., Siegel, D.A., Thunell, R., 2009. Rapid downward transport of the neurotoxin domoic acid in coastal waters. Nature Geosci. 2 (4), 272–275.
Sekula-Wood, E., Benitez-Nelson, C., Morton, S., Anderson, C., Burrell, C., Thunell, R., 2011. *Pseudo-nitzschia* and domoic acid fluxes in Santa Barbara Basin (CA) from 1993 to 2008. Harm. Algae 10 (6), 567–575.
Shanks, A.L., Edmondson, E.W., 1989. Laboratory-made artificial marine snow: a biological model of the real thing. Mar. Biol. 101, 463–470.
Shanks, A.L., Trent, J.D., 1980. Marine snow: sinking rates and potential role in vertical flux. Deep Sea Res. Part A. Oceanogr. Res. Pap. 27 (2), 137–143.
Silver, M.W., Shanks, A.L., Trent, J.D., 1978. Marine Snow: microplankton habitat and source of small-scale patchiness in pelagic populations. Science 201 (4353), 371–373.
Simon, M., Grossart, H.-P., Schweitzer, B., Ploug, H., 2002. Microbial ecology of organic aggregates in aquatic ecosystems. Aquat. Microb. Ecol. 28 (2), 175–211.
Sison-Mangus, M.P., Jiang, S., Tran, K.N., Kudela, R.M., 2014. Host-specific adaptation governs the interaction of the marine diatom, *Pseudo-nitzschia* and their microbiota. ISME J. 8 (1), 63–76.
Smetacek, V.S., 1985. Role of sinking in diatom life history-cycles: ecological, evolutionary and geological significance. Mar. Biol. 84, 239–251.
StatSoft, I., 2002. STATISTICA for Windows, Statistica 6.1 Ed.. StatSoft, Inc., Tulsa, OK.
Tammilehto, A., Nielsen, T.G., Krock, B., Møller, E.F., Lundholm, N., 2012. *Calanus* spp.—vectors for the biotoxin, domoic acid, in the Arctic marine ecosystem? Harm. Algae 20, 165–174.
Tatters, A.O., Fu, F.-X., Hutchins, D.A., 2012. High CO_2 and silicate limitation synergistically increase the toxicity of *Pseudo-nitzschia fraudulenta*. PLoS One 7 (2), e32116.
Tester, P., Pan, Y., Doucette, G.J., 2001. In: Hallegraef, G.M., Blackburn, S.I., Bolch, C.J., Lewis, R.J. (Eds.), Accumulation of Domoic Acid Activity in Copepods. Intergovernmental Oceanographic Commission of UNESCO, France, pp. 418–420.
Thornton, D., 2002. Diatom aggregation in the sea: mechanisms and ecological implications. Eur. J. Phycol. 37 (2), 149–161.
Trainer, V.L., Adams, N.G., Bill, B.D., Stehr, C.M., Wekell, J.C., Moeller, P., Busman, M., Woodruff, D., 2000. Domoic acid production near California coastal upwelling zones, june 1998. Limnol. Oceanogr. 45 (8), 1818–1833.
Trainer, V.L., Bates, S.S., Lundholm, N., Thessen, A.E., Cochlan, W.P., Adams, N.G., Trick, C.G., 2012. *Pseudo-nitzschia* physiological ecology, phylogeny, toxicity, monitoring and impacts on ecosystem health. Harm. Algae 14, 271–300.
Turner, J.T., 2015. Zooplankton fecal pellets, marine snow, phytodetritus and the ocean's biological pump. Prog. Oceanogr. 130, 205–248.
Utermöhl, H., 1958. Zur Vervollkommung der quantitativen Phytoplankton Methodik. Mitt. internat. Verein. Limnol. 9, 1–38.
Vigilant, V., Silver, M.W., 2005. Domoic acid in the fat innkeeper worm, Urechis caupo, at Elkhorn Slough, CA. 3rd Symposium for Harmful Algae in the US, Monterey, CA.
Vigilant, V.L., Silver, M., 2007. Domoic acid in benthic flatfish on the continental shelf of Monterey Bay, California, USA. Mar. Biol. 151 (6), 2053–2062.
Vojvoda, J., Lamy, D., Sintes, E., Garcia, J.A.L., Turk, V., Herndl, G.J., 2014. Seasonal variation in marine-snow-associated and ambient-water prokaryotic communities in the northern Adriatic Sea. Aquat. Microb. Ecol. 73 (3), 211–224.
Wells, M.L., Trick, C.G., Cochlan, W.P., Hughes, M.P., Trainer, V.L., 2005. Domoic acid: the synergy of iron, copper, and the toxicity of diatoms. Limnol. Oceanogr. 50 (6), 1908–1917.
Wells, M.L., Trainer, V.L., Smayda, T.J., Karlson, B.S.O., Trick, C.G., Kudela, R.M., Ishikawa, A., Bernard, S., Wulff, A., Anderson, D.M., Cochlan, W.P., 2015. Harmful algal blooms and climate change: learning from the past and present to forecast the future. Harm. Algae 49, 68–93.
Welschmeyer, N.A., 1994. Fluorometric analysis of chlorophyll *a* in the presence of chlorophyll *b* and pheopigments. Limnol. Oceanogr. 39 (8), 1985–1992.
Wright, J.L.C., Boyd, R.K., de Freitas, A.S.W., Falk, M., Foxall, R.A., Jamieson, W.D., Laycock, M.V., McCulloch, A.W., McInnes, A.G., Odense, P., Pathak, V.P., Quilliam, M.A., Ragan, M.A., Sim, P.G., Thibault, P., Walter, J.A., Gilgan, M., Richard, D.J.A., 1989. Identification of domoic acid, a neuroexcitatory amino acid, in toxic mussels from Eastern Prince Edward Island. Can. J. Chem. 67, 481–490.
Zabaglo, K., Chrapusta, E., Bober, B., Kaminski, A., Adamski, M., Bialczyk, J., 2016. Environmental roles and biological activity of domoic acid: a review. Algal Res. 13, 94–101.